Supplementary Figure S1

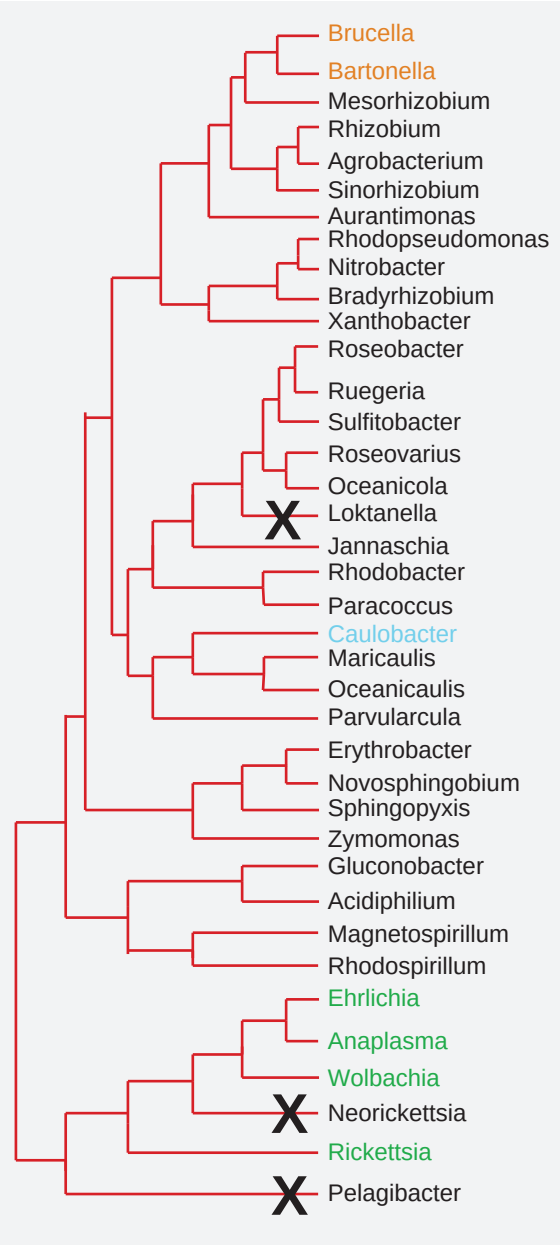

Conservation of the PopZ coding sequence through *Alphaproteobacterial* lineages. The diagram depicts a species tree of the *Alphaproteobacteria*, taken from the construction by Williams et al. (2007), and based on Bayesian analysis of consensus alignments for 104 protein families. The branches end at the level of Genus. PopZ homologs were identified in all branches of the tree with the exception of *Loktanella*, *Neorickettsia*, and *Pelagibacter* (gene loss is indicated by an X). Genera discussed in detail in Supplementary Figure 2 are highlighted in color.

Williams, K.P., Sobral, B.W., Dickerman, A.W. (2007) A robust species tree for the alphaproteobacteria. *J Bacteriol* **189**: 4578–4586

Supplementary Figure S2

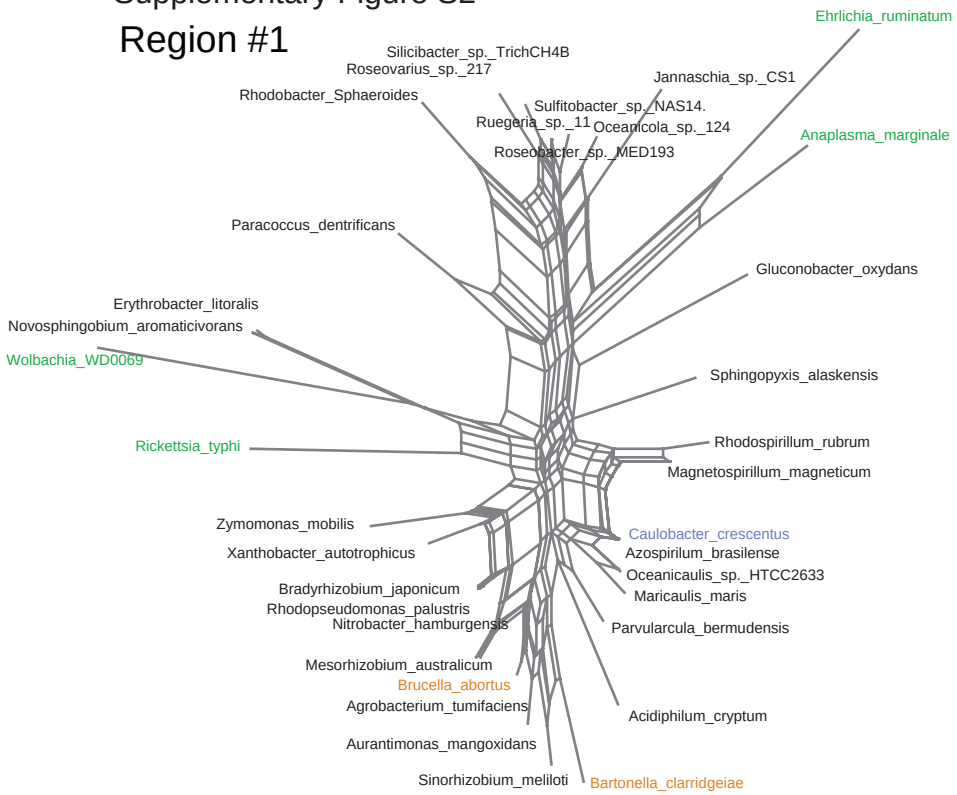

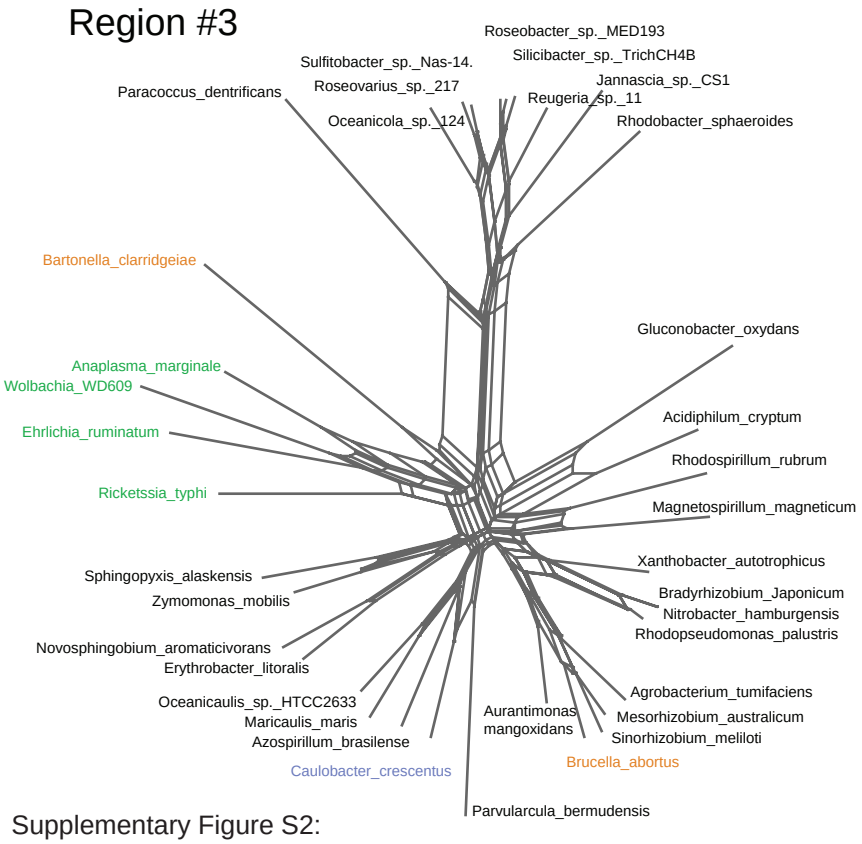

Caulobacter_crescentus MEEILASIRRIISED

Ehrlichia_ruminatum IKDVIANIRKVMSSN

Anaplasma_marginale IRDVVASIRKVILSD

Wolbachia_WD0069 VKDILEDIKKAISGK

Rickettsia_typhi IEEILKSIKGIINEH

Brucella_abortus MEEILASIRRIIEDS

Bartonella_clarridgeiae MDEILTSIREIIEEN

Caulobacter_crescentus
TLEDVVRELLRPLLKEWLDQNLPRIVETKVEEEVQRISR

Ehrlichia_ruminatum
TIEELVISILKPELSTWLNNNLQKIVQDIVEREIKHIVK

Anaplasma_marginale
TVEELTLSVLRPQLSEWLNENLPGLVREIVEREIGKLIK

Wolbachia_WD0069
TVEELVTSLLKPQLSEWLNKYLHALVKEVVEKELKDIIN

Rickettsia_typhi
ALEELVIEMLKPELKVWLDKNLPILVKELVEIEIKKLVQ

Brucella_abortus
SFDEIAAELLRPMLQDWLDKNLPTLVERLVREEIERVVR

Bartonella_clarridgeiae
SAEKVARDVLRPAIAEWLQCQLPILLEKILREEIVKTLK

Supplementary Figure S2:
Phylogenetic tree diagrams for conserved regions in PopZ. The Splitstree4 software package (Huson and Bryant, 2006) was used to create unrooted networks that show the divergence of PopZ coding sequences across alphaproteobacterial phyla. The most conserved sequence regions within R1 (top panel) and R3 (bottom panel) were taken from one representative of each genus (Supplementary Figure 1) and used to make two separate trees. Members of the Rickettsiales order (highlighted in green) have divergent R1 sequences but similar R3 sequences. Conversely, two members of the Rhizobiales order, Bartonella and Brucella (highlighted in orange) have similar R1 sequences but divergent R3 sequences. The relevant amino acid sequences for these species (and also Caloubacter crescentus) are shown on the right side of the tree diagram. These different patterns of phylogenetic conservation indicate that a significant fraction of the residues in R1 and R3 are not necessarily co-conserved, and that these regions of PopZ are evolving under different processes that do not generate identical tree signals.

D.H. Huson and D. Bryant, Application of Phylogenetic Networks in Evolutionary Studies, Molecular Biology and Evolution, 23(2):254-267, 2006. Software available from www.splitstree.org.

Supplementary Figure S3

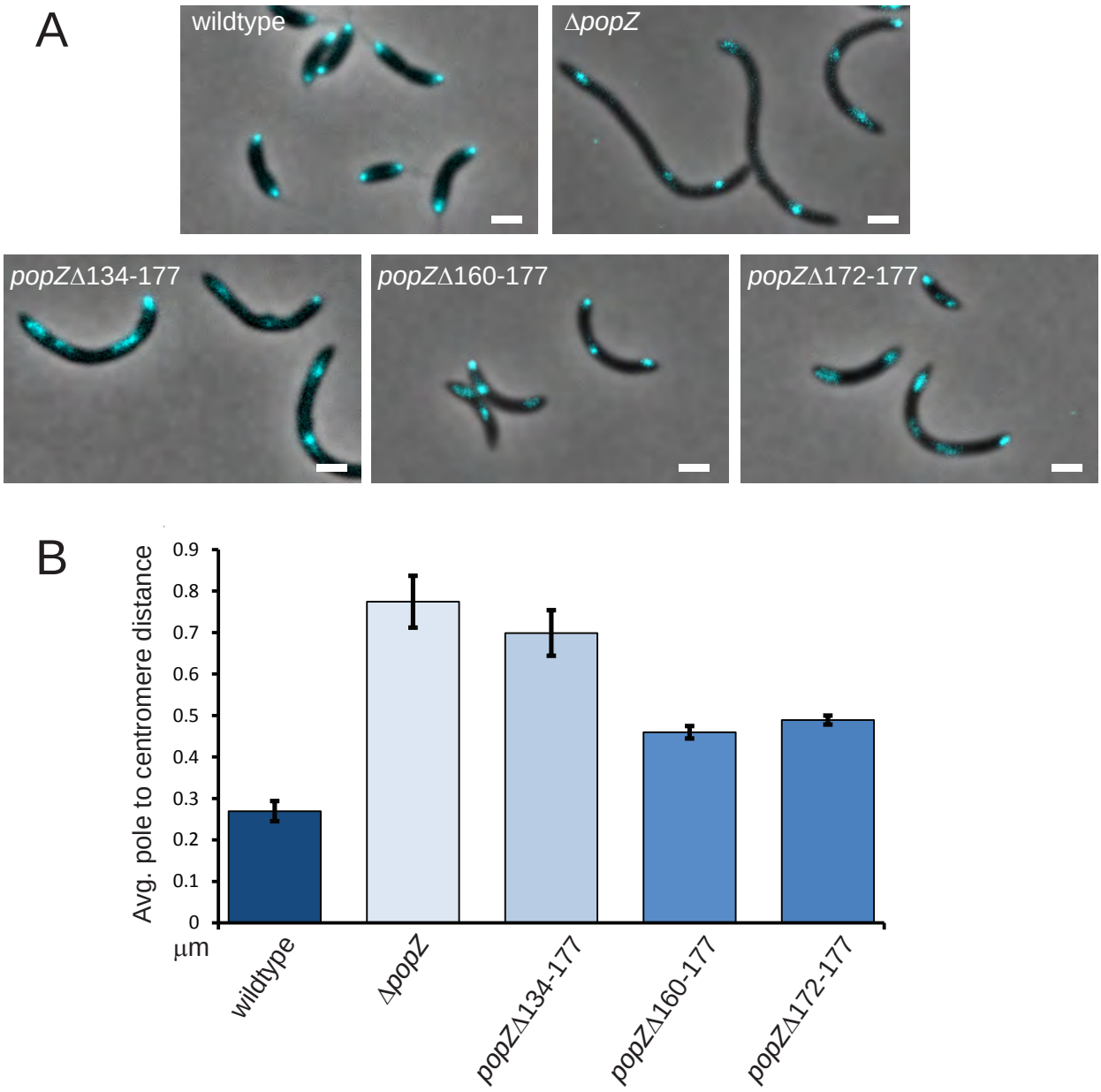

Centromere anchoring is inhibited in PopZ C-terminal truncation mutants.

A) Centromere position was observed in live cells in which the centromere binding protein MipZ was replaced with MipZ-CFP. In each strain, an untagged copy of wildtype *popZ* or the indicated *popZ* truncation mutant is expressed from the endogenous popZ promoter. Representative images from strains GB1107, GB1113, GB1127, GB1128, and GB1129 are shown. Fluorescence images are overlayed on pahse contrast images. Bar = 1μm. B) The distance between a cell pole and the nearest centromere was calculated by drawing a straight line between the centroid of the MipZ-CFP focus and the contrast edge at the cell pole in the phase contrast image. Cells with only one centromere were omitted from the analysis. At least 100 cells (200 cell poles) of each genotype in A were quantified per experiment. The error bars represent the standard deviation of the average value calculated from three independent experiments.

Supplementary Figure S4

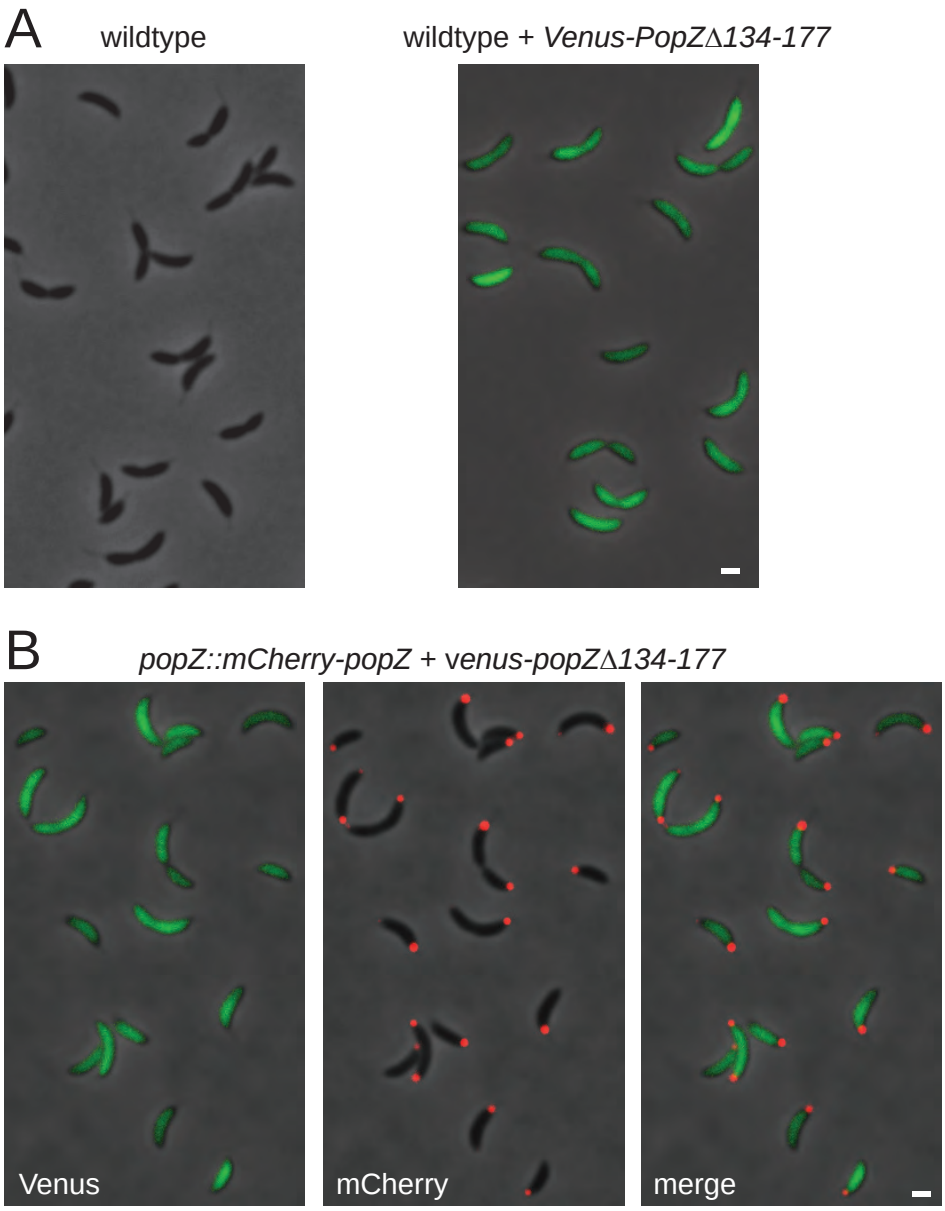

Diffusely localized venus-popZΔ134-177 does not have a dominant negative effect on PopZ activty.

A) Venus-popZΔ134-177 was expressed in a wildtype background (GB1121). The length of wildtype cells (left panel) is not changed after adding the venus-popZΔ134-177expression plasmid (righ panel), indicating that the N-terminal 133 amino acids of PopZ do not act as a dominant negative for inhibiting cell division. B) The venus-popZΔ134-177 expression plasmid was transformed into cells expressing full length mCherry-PopZ (GB1122). Polar localization of full length mCherry-PopZ was not perturbed. Where appllicable, a fluorescence image is overlayed on a phase contrast image. Bar = 1 μm.

Supplementary Figure S5

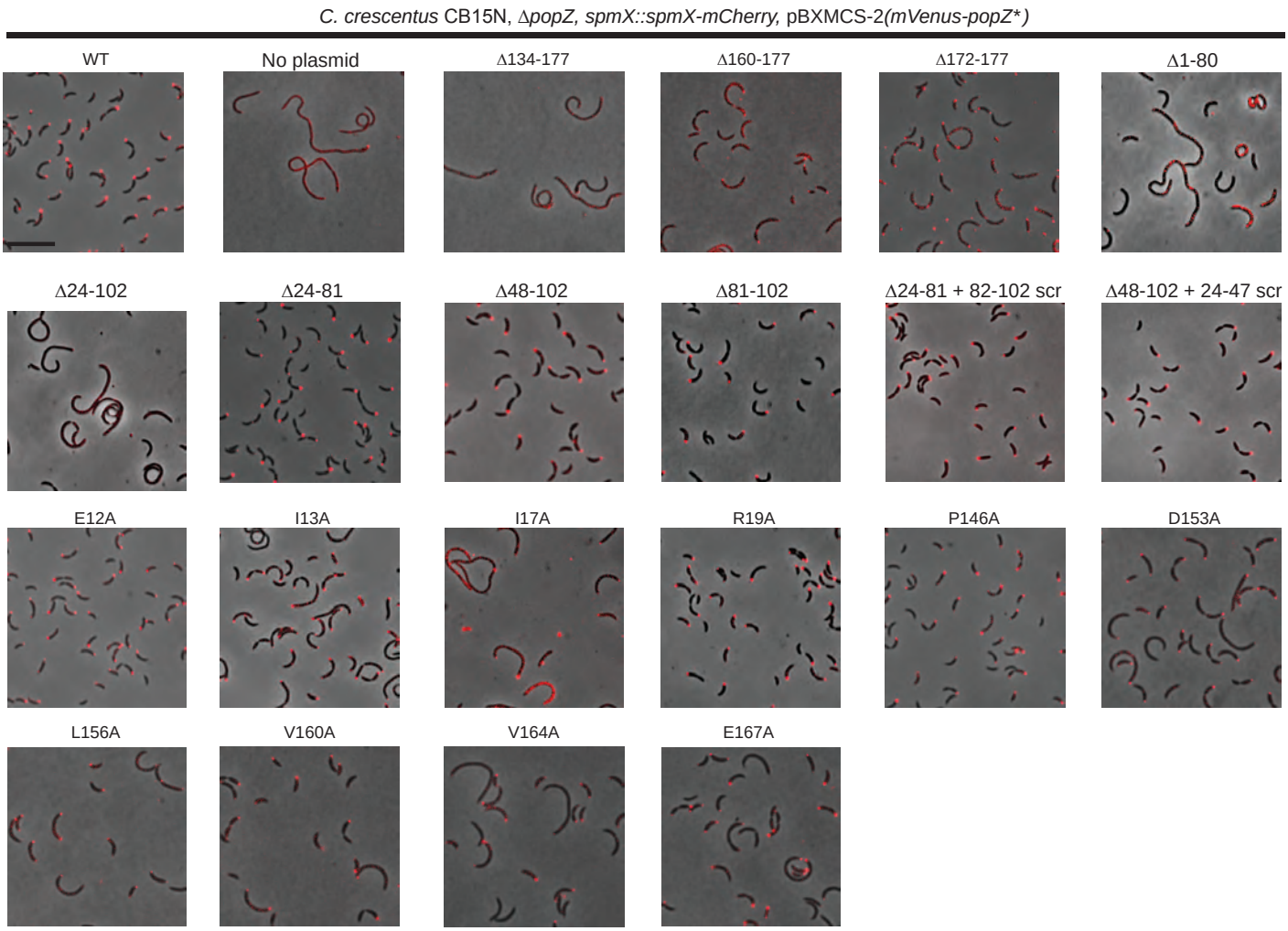

Localization of SpmX-mCherry in PopZ variant backgrounds.

Spmx-mCherry fluorescence (red) overlays the phase contrast image (grayscale). Bar = 9 μm.
Representative images from AP253, AP236, AP280, AP300, AP282, AP299, AP254, AP257, AP298, AP342, AP343, AP344, AP292, AP293, AP290, AP291, AP283, AP285, AP286, AP287, AP288, and AP289 are presented.
Corresponding quantitation of polar SpmX-mCherry localization is presented in graphs in the main text figures.

Supplemental Figure S6

C. crescentus CB15N, Δ*popZ,* pBXMCS-2*(mVenus-popZ*)*

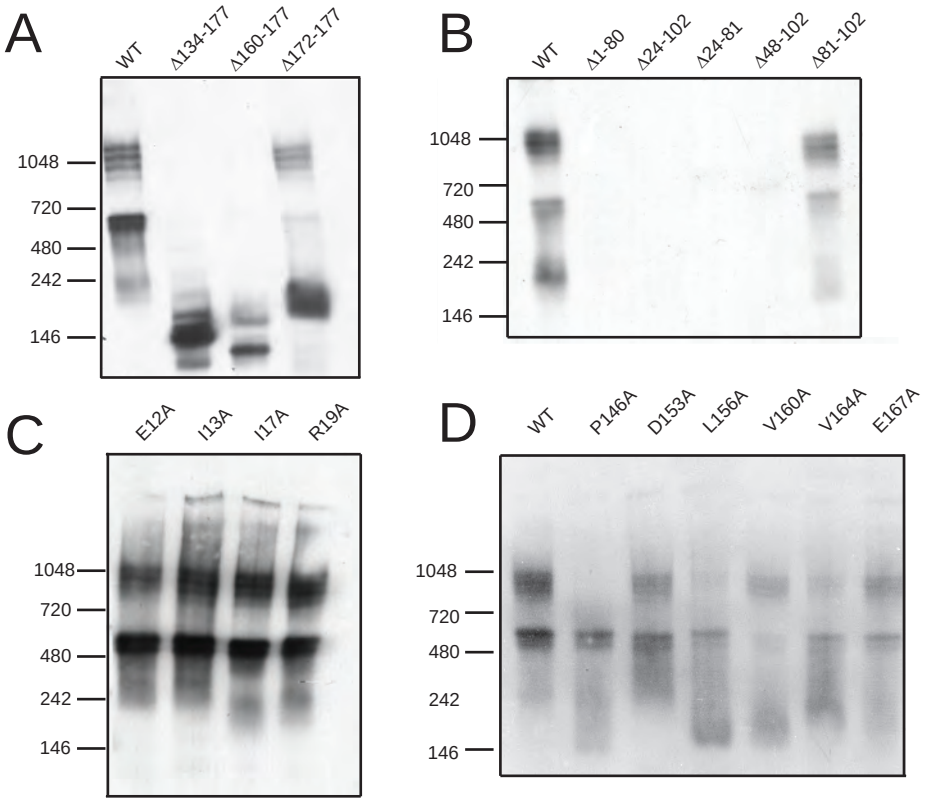

Electrophoretic migration of venus-tagged PopZ variant proteins.

Whole cell lysates of venus-tagged PopZ expressing strains in Figure 3B (A), Figure 4B (B) Figure 5B (C), and Figure 6B (D) of the main text were resolved native gels, then probed with anti-PopZ antisera by immunoblotting.

Supplementary Figure S7

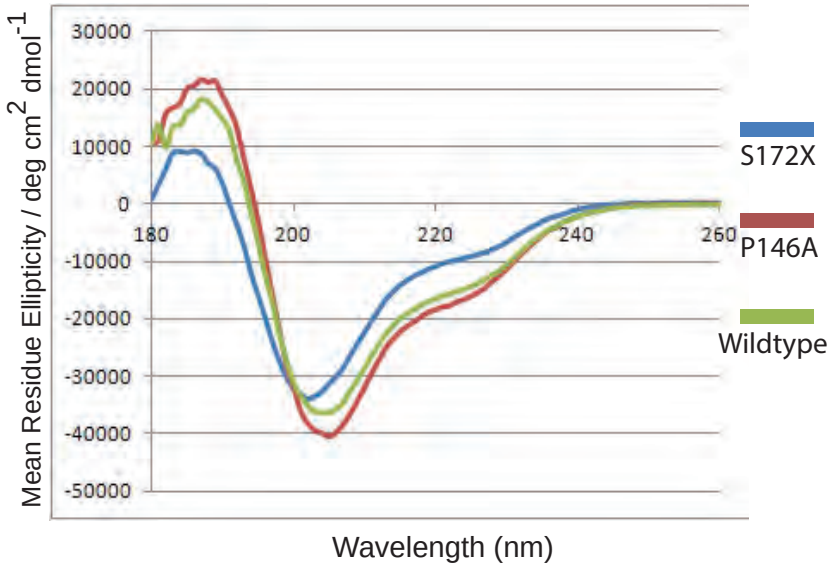

Circular dichroism analysis. Individual uv-CD spectra for purified wildtype, P146A, and PopZΔ172-177 proteins are compared by overlay. A positive band at 190 nm and negative bands at 208 nm and 222 nm are characteristic alpha helical signatures. The shift in the minimum to shorter wavelengths (203 nm for PopZΔ172-177 and 205nm for PopZ P146A and wildtype) are inidicative of the influence of disordered regions, which have a minimum signal at 200nm (Chemes et al. 2012).

Chemes, L.B., Alonso, L.G., Noval, M.G., Prat-Gay, G. de (2012). Circular dichroism techniques for the analysis of intrinsically disordered proteins and domains. *Methods Mol Biol* **895**: 387–404

Supplementary Figure S8

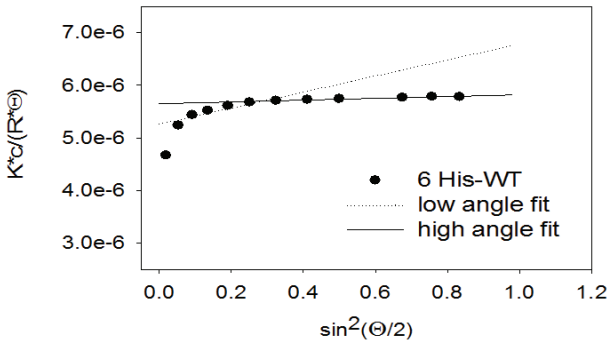

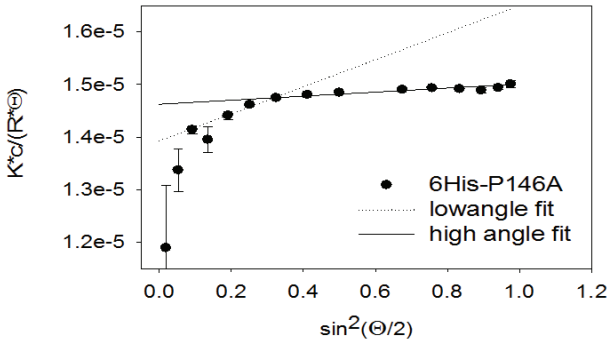

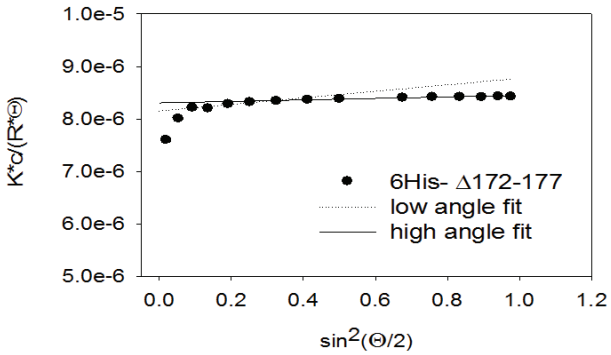

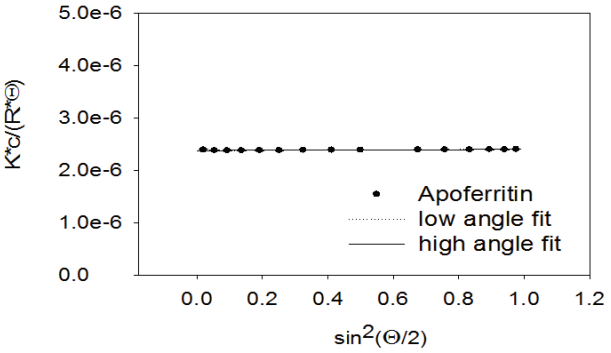

Illustration of non-linear angular dependence of scattered light for PopZ protein oligomers. A plot of K*c /R(Θ) vs. $\sin^2(\Theta/2)$, a Zimm plot (Zimm, 1948), yields a curve whose intercept gives $(Mw)^{-1}$ and whose slope gives root-mean-square radius (rms), also known as radius of gyration, Rg, which characterizes particle dimensions independently of particle shape. Shown are Zimm plots for apexes of eluting peaks. Two separate curves are generated from data obtained generated by high or low angle incident light. In heterogenous samples, the data from lower angles is primarily influenced by the largest particles. The angular dependence of the wildtype and PopZ P146A samples is more skewed than the PopZΔ172-177 sample, indicating qualitative differences in the distributions of particle size. The Apoferritin control, which is uniform in particle size, is linear across all angles. Results of MW and rms determinations at higher angles are summarized in Table 1.

Zimm B H (1948) Apparatus and Methods for Measurement and Interpretation of the Angular Variation of Light Scattering; Preliminary Results on Polystyrene Solutions. *J.Chem.Phys*. **16**; 1099-1116

Supplementary Table 1:	**Bacterial strains**	
***C. crescentus* strains**	**Relevant genotype/description**	**Construction, source or reference**
AP236	*spmX:: spmX mCherry; popZ::Δ*	Bowman *et al.* (2010)
AP253	*spmX:: spmX mCherry; popZ::Δ; pBXMCS-2 + mVenus PopZ*	pAP214 electroporated into AP236
AP254	*spmX:: spmX mCherry; popZ::Δ; pBXMCS-2 + mVenus PopZ Δ24–102*	pAP237 electroporated into AP236
AP257	*spmX:: spmX mCherry; popZ::Δ; pBXMCS-2 + mVenus PopZ Δ24–81*	pAP240 electroporated into AP236
AP280	*spmX:: spmX mCherry; popZ::Δ; pBXMCS-2 + mVenus PopZ Δ134–177*	pAP259 electroporated into AP236
AP282	*spmX:: spmX mCherry; popZ::Δ; pBXMCS-2 + mVenus PopZ Δ172–177*	pAP261 electroporated into AP236
AP283	*spmX:: spmX mCherry; popZ::Δ; pBXMCS-2 + mVenus PopZ P146A*	pAP262 electroporated into AP236
AP285	*spmX:: spmX mCherry; popZ::Δ; pBXMCS-2 + mVenus PopZ D153A*	pAP264 electroporated into AP236
AP286	*spmX:: spmX mCherry; popZ::Δ; pBXMCS-2 + mVenus PopZ L156A*	pAP265 electroporated into AP236
AP287	*spmX:: spmX mCherry; popZ::Δ; pBXMCS-2 + mVenus PopZ V160A*	pAP266 electroporated into AP236
AP288	*spmX:: spmX mCherry; popZ::Δ;pBXMCS-2 + mVenus PopZ V164A*	pAP267 electroporated into AP236
AP289	*spmX:: spmX mCherry; popZ::Δ;pBXMCS-2 + mVenus PopZ E167A*	pAP268 electroporated into AP236
AP290	*spmX:: spmX mCherry; popZ::Δ; pBXMCS-2 + mVenus PopZ I13A*	pAP269 electroporated into AP236

AP291	*spmX:: spmX mCherry; popZ::Δ; pBXMCS-2 + mVenus PopZ I17A*	pAP270 electroporated into AP236
AP292	*spmX:: spmX mCherry; popZ::Δ; pBXMCS-2 + mVenus PopZ E12A*	pAP272 electroporated into AP236
AP293	*spmX:: spmX mCherry; popZ::Δ; pBXMCS-2 + mVenus PopZ R19A*	pAP271 electroporated into AP236
AP298	*spmX:: spmX mCherry; popZ::Δ; pBXMCS-2 + mVenus PopZ Δ81–102*	pAP277 electroporated into AP236
AP299	*spmX:: spmX mCherry; popZ::Δ; pBXMCS-2 + mVenus PopZ Δ1–80*	pAP278 electroporated into AP236
AP300	*spmX:: spmX mCherry; popZ::Δ; pBXMCS-2 + mVenus PopZ Δ160–177*	pAP279 electroporated into AP236
AP302	*popZ::Δ; pBXMCS-2 + mVenus PopZ Δ48–102*	pAP301 electroporated into GB255
AP303	*popZ::Δ; pBXMCS-2 + mVenus PopZ Δ134–177*	pAP259 electroporated into GB255
AP305	*popZ::Δ; pBXMCS-2 + mVenus PopZ Δ172–177*	pAP261 electroporated into GB255
AP306	*popZ::Δ; pBXMCS-2 + mVenus PopZ P146A*	pAP262 electroporated into GB255
AP308	*popZ::Δ; pBXMCS-2 + mVenus PopZ D153A*	pAP264 electroporated into GB255
AP309	*popZ::Δ; pBXMCS-2 + mVenus PopZ L156A*	pAP265 electroporated into GB255
AP310	*popZ::Δ; pBXMCS-2 + mVenus PopZ V160A*	pAP266 electroporated into GB255
AP311	*popZ::Δ; pBXMCS-2 + mVenus PopZ V164A*	pAP267 electroporated into GB255
AP312	*popZ::Δ; pBXMCS-2 + mVenus PopZ E167A*	pAP268 electroporated into GB255
AP313	*popZ::Δ; pBXMCS-2 + mVenus PopZ I13A*	pAP269 electroporated into GB255
AP314	*popZ::Δ; pBXMCS-2 + mVenus PopZ I17A*	pAP270 electroporated into GB255
AP315	*popZ::Δ; pBXMCS-2 + mVenus PopZ E12A*	pAP272 electroporated into GB255
AP316	*popZ::Δ; pBXMCS-2 + mVenus PopZ R19A*	pAP271 electroporated into GB255

AP320	*popZ::Δ; pBXMCS-2 + mVenus PopZ Δ81–102*	pAP277 electroporated into GB255
AP321	*popZ::Δ; pBXMCS-2 + mVenus PopZ Δ1–80*	pAP278 electroporated into GB255
AP322	*popZ::Δ; pBXMCS-2 + mVenus PopZ Δ160–177*	pAP279 electroporated into GB255
AP323	*popZ::Δ; pBXMCS-2 + mVenus PopZ*	pAP214 electroporated into GB255
AP324	*popZ::Δ; pBXMCS-2 + mVenus PopZ Δ24–102*	pAP237 electroporated into GB255
AP327	*popZ::Δ; pBXMCS-2 + mVenus PopZ Δ24–81*	pAP240 electroporated into GB255
AP342	*spmX:: spmX mCherry; popZ::Δ; pBXMCS-2 + mVenus PopZ Δ48–102*	pAP301 electroporated into AP236
AP343	*spmX:: spmX mCherry; popZ::Δ; pBXMCS-2 + mVenus PopZ Δ48–102 + 24-47 scr*	pAP332 electroporated into AP236
AP344	*spmX:: spmX mCherry; popZ::Δ; pBXMCS-2 + mVenus PopZ Δ24–81 + 82-102 scr*	pAP333 electroporated into AP236
CB15N	Synchronizeable derivative of WT CB15	Evinger and Agabian (1977)
GB135	*popZ::popZ-FLAG*	Bowman *et al.* (2008)
GB255	*popZ::Δ*	Bowman *et al.* (2008)
GB544	*popZ::Δ; vanA::mCherry-popZ R1*	pGB525 mated into GB255
GB545	*popZ::Δ; vanA::mCherry-popZ R2*	pGB526 mated into GB255
GB750	*popZ::Δ; vanA::mCherry-popZ R3*	pGB527 mated into GB255
GB757	*popZ::popZ-FLAG; pBXMCS-2 + mCherry-PopZ R1*	pGB570 electroporated into GB135
GB758	*popZ::popZ-FLAG; pBXMCS-2 + mCherry-PopZ R3*	pGB572 electroporated into GB135
GB885	*popZ::popZ Δ134–177*	pGB844 mated into GB255
GB886	*popZ::popZ Δ160–177*	pGB845 mated into GB255
GB888	*popZ::popZ Δ172–177*	pGB823 mated into GB255
GB890	*popZ::popZ P146A*	pGB822 mated into GB255

GB892	*popZ::popZ D153A*	pGB848 mated into GB255
GB893	*popZ::popZ L156A*	pGB849 mated into GB255
GB894	*popZ::popZ V160A*	pGB850 mated into GB255
GB895	*popZ::popZ V164A*	pGB851 mated into GB255
GB896	*popZ::popZ E167A*	pGB852 mated into GB255
GB897	*popZ::popZ I13A*	pGB853 mated into GB255
GB898	*popZ::popZ I17A*	pGB854 mated into GB255
GB899	*popZ::popZ E12A*	pGB855 mated into GB255
GB900	*popZ::popZ R19A*	pGB856 mated into GB255
GB1007	*popZ::mCherry-PopZ*	pPD 72 mated into GB255
GB1078	*popZ::Δ; vanA::mCherry-popZ*	pGB528 mated into GB255
GB1107	*mipZ::mipZ-CFP*	Goley *et al.* (2011)
GB1113	*mipZ::mipZ-CFP; popZ::Δ*	*popZ::Δ* transduced from GB255 into GB113
GB1115	*popZ::popZ Δ1–80*	pGB1108 mated into GB255
GB1116	*popZ::popZ Δ24–81*	pGB1109 mated into GB255
GB1117	*popZ::popZ Δ24–102*	pGB1110 mated into GB255
GB1118	*popZ::popZ Δ48–102*	pGB1111 mated into GB255
GB1119	*popZ::popZ Δ81–102*	pGB1112 mated into GB255
GB1121	*pBXMCS-2 + mVenus PopZ Δ134–177*	pAP259 electroporated into CB15N
GB1122	*popZ::mCherry-popZ; pBXMCS-2 + mVenus PopZ Δ134–177*	pAP259 electroporated into GB1007
GB1127	*mipZ::mipZ-CFP; popZ::Δ134–177*	*popZ::Δ134–177* transduced from GB855 into GB113
GB1128	*mipZ::mipZ-CFP; popZ::Δ160–177*	*popZ::Δ160–177* transduced from GB856 into GB113
GB1129	*mipZ::mipZ-CFP; popZ::Δ172–177*	*popZ::Δ172–177* transduced from GB888 into GB113
***E. coli* stains**	**Relevant genotype/description**	**Source**
Rosetta	High protein expression	Novagen
GB169	*pET28a + PopZ*	Cloned into pET28a via 5' NdeI and 3' EcoRI sites
GB923	*pET28a + PopZ P146A*	Cloned into pET28a via 5' NdeI and 3' EcoRI sites

GB924	*pET28a + PopZ Δ172–177*	Cloned into pET28a via 5' NdeI and 3' EcoRI sites

Bowman, G.R., Comolli, L.R., Gaietta, G.M., Fero, M., Hong, S.-H., Jones, Y., Lee, J.H., Downing, K.H., Ellisman, M.H., McAdams, H.H., Shapiro, L. (2010) *Caulobacter* PopZ forms a polar subdomain dictating sequential changes in pole composition and function. *Mol Microbiol* **76**: 173–189

Bowman, G.R., Comolli, L.R., Zhu, J., Eckart, M., Koenig, M., Downing, K.H., Moerner, W.E., Earnest, T., Shapiro, L. (2008) A polymeric protein anchors the chromosomal origin/ParB complex at a bacterial cell pole. *Cell* **134**: 945–955

Evinger, M., Agabian, N. (1977) Envelope-associated nucleoid from *Caulobacter crescentus* stalked and swarmer cells. *J Bacteriol* **132**: 294–301

Goley, E.D., Yeh, Y.-C., Hong, S.-H., Fero, M.J., Abeliuk, E., McAdams, H.H., Shapiro, L. (2011) Assembly of the *Caulobacter* cell division machine. *Mol Microbiol* **80**: 1680–1698

Supplementary Table 2: Plasmids

Plasmids	**Description**	**Backbone**	**Source**
pBXMCS-2	High copy replicating plasmid	pBXMCS-2	Thianbichler *et al.* (2007)
pMCS-4	Integrating plasmid	pMCS-4	Thianbichler *et al.* (2007)
pAP214	High copy *PxylX-mVenus-PopZ*	pBXMCS-2	This study
pAP237	High copy *PxylX-mVenus-PopZ Δ24–102*	pBXMCS-2	This study
pAP240	High copy *PxylX-mVenus-PopZ Δ24–81*	pBXMCS-2	This study
pAP259	High copy *PxylX-mVenus-PopZ Δ134–177*	pBXMCS-2	This study
pAP261	High copy *PxylX-mVenus-PopZ Δ172–177*	pBXMCS-2	This study

pAP262	High copy *PxylX-mVenus-PopZ P146A*	pBXMCS-2	This study
pAP264	High copy *PxylX-mVenus-PopZ D153A*	pBXMCS-2	This study
pAP265	High copy *PxylX-mVenus-PopZ L156A*	pBXMCS-2	This study
pAP266	High copy *PxylX-mVenus-PopZ V160A*	pBXMCS-2	This study
pAP267	High copy *PxylX-mVenus-PopZ V164A*	pBXMCS-2	This study
pAP268	High copy *PxylX-mVenus-PopZ E167A*	pBXMCS-2	This study
pAP269	High copy *PxylX-mVenus-PopZ I13A*	pBXMCS-2	This study
pAP270	High copy *PxylX-mVenus-PopZ I17A*	pBXMCS-2	This study
pAP271	High copy *PxylX-mVenus-PopZ E12A*	pBXMCS-2	This study
pAP272	High copy *PxylX-mVenus-PopZ R19A*	pBXMCS-2	This study
pAP277	High copy *PxylX-mVenus-PopZ Δ81–102*	pBXMCS-2	This study
pAP278	High copy *PxylX-mVenus-PopZ Δ1–80*	pBXMCS-2	This study
pAP279	High copy *PxylX-mVenus-PopZ Δ160–177*	pBXMCS-2	This study
pAP301	High copy *PxylX-mVenus-PopZ Δ48–102*	pBXMCS-2	This study
pAP332	High copy *PxylX-mVenus-PopZ Δ48–102 + 24-47 scr*	pBXMCS-2	This study

pAP333	High copy *PxylX-mVenus-PopZ Δ24–81 + 82-102 scr*	pBXMCS-2	This study
pGB525	*PvanA-mCherry-popZ R1*integrates at *vanA* locus	pVCHYN-2	This study
pGB526	*PvanA-mCherry-popZ R2* integrates at *vanA* locus	pVCHYN-2	This study
pGB527	*PvanA-mCherry-popZ R3* integrates at *vanA* locus	pVCHYN-2	This study
pGB528	*PvanA-mCherry-popZ* integrates at *vanA* locus	pVCHYN-2	This study
pGB570	High copy *PxylX-mCherry-PopZ R1*	pBXMCS-2	This study
pGB572	High copy *PxylX-mCherry-PopZ R3*	pBXMCS-2	This study
pGB822	*PpopZ-PopZ P146A* integrates at *popZ* locus	pMCS-4	This study
pGB823	*PpopZ-PopZ Δ172–177* integrates at *popZ* locus	pMCS-4	This study
pGB844	*PpopZ-PopZ Δ134–177* integrates at *popZ* locus	pMCS-4	This study
pGB845	*PpopZ-PopZ Δ160–177* integrates at *popZ* locus	pMCS-4	This study
pGB848	*PpopZ-PopZ D153A* integrates at *popZ* locus	pMCS-4	This study
pGB849	*PpopZ-PopZ L156A* integrates at *popZ* locus	pMCS-4	This study
pGB850	*PpopZ-PopZ V160A* integrates at *popZ* locus	pMCS-4	This study

pGB851	*PpopZ-PopZ V164A* integrates at *popZ* locus	pMCS-4	This study
pGB852	*PpopZ-PopZ E167A* integrates at *popZ* locus	pMCS-4	This study
pGB853	*PpopZ-PopZ I13A* integrates at *popZ* locus	pMCS-4	This study
pGB854	*PpopZ-PopZ I17A* integrates at *popZ* locus	pMCS-4	This study
pGB855	*PpopZ-PopZ E12A* integrates at *popZ* locus	pMCS-4	This study
pGB856	*PpopZ-PopZ R19A* integrates at *popZ* locus	pMCS-4	This study
pGB1108	*PpopZ-PopZ Δ1–80* integrates at *popZ* locus	pMCS-4	This study
pGB1109	*PpopZ-PopZ Δ24–81* integrates at *popZ* locus	pMCS-4	This study
pGB1110	*PpopZ-PopZ Δ24–102* integrates at *popZ* locus	pMCS-4	This study
pGB1111	*PpopZ-PopZ Δ48–102* integrates at *popZ* locus	pMCS-4	This study
pGB1112	*PpopZ-PopZ Δ81–102* integrates at *popZ* locus	pMCS-4	This study
pPD72	*PpopZ-mCherry-PopZ* integrates at *popZ* locus	pMCS-4	This study

Thanbichler, M., Iniesta, A.A., Shapiro, L. (2007) A comprehensive set of plasmids for vanillate- and xylose-inducible gene expression in *Caulobacter crescentus*. *Nucleic Acids Res* **35**: e137